Mechanical Spectrometry of the β-Relaxation in Poly(methyl methacrylate)

E. Muzeau,[‡] J. Perez,[‡] and G. P. Johari*,[†]

Department of Materials Science and Engineering, McMaster University, Hamilton, Ontario L8S 4L7, Canada, and Groupe d'Etude de Métallurgie Physique et Physique des Matériaux, Institut National des Sciences Appliquées, URA CNRS 341, 69621 Villeurbanne Cedex, France

Received January 2, 1991; Revised Manuscript Received April 4, 1991

ABSTRACT: Shear modulus and loss spectra of poly(methyl methacrylate) (PMMA) have been measured over a frequency range from 2×10^{-4} to 1 Hz and under isothermal conditions at temperatures from 200 to 300 K, and similar measurements have been made for fixed frequencies of 0.1 and 1 Hz in the temperature range of its β-relaxation. The height of the β-relaxation peak increases with increase in the temperature, and its rate is described according to the Arrhenius and Eyring equations. The spectra of mechanical loss are asymmetric and broader at the high-frequency side despite the contributions, which are significant at the low-frequency side or at high temperatures, from the α-relaxation process. The shape of the spectra has been analyzed in terms of (i) a stretched exponential or Kohlrausch–Williams–Watts relaxation function and (ii) a Gaussian distribution function modified to introduce asymmetry in a relaxation spectrum. A procedure for the analysis of the real and imaginary components of the elastic modulus has been developed for both functions and used to obtain the strength of the β-relaxation process. The modified Gaussian distribution allows an interpretation in terms of the distribution of activation entropies and enthalpies and a self-consistent description of the isothermal spectra and of the mechanical relaxation data measured for a fixed frequency but at different temperatures. The dielectric relaxation rate for the β-process is the same as the mechanical relaxation rate over a wide range of temperature. Theoretical implications of these observations of the mechanical spectra for our concepts of localized relaxation in amorphous materials have been discussed, and it is argued that the frequency-independent background loss in PMMA is negligible or zero.

I. Introduction

The persistence of localized molecular motions in the glassy state of materials is now recognized as an intrinsic property of the disordered structure,[1,2] where frozen-in density fluctuations produce "islands of mobility",[3] i.e., regions of low or high density.[4] In a recent theoretical development[5] aimed at understanding the nature of these localized motions in terms of defects or "soft sites", it is assumed that the stress-biased perturbations become concentrated at these local sites and that the magnitude of these perturbations increases, within the hierarchical constraints, with the time of the application of the stress. Thus the stress-biased perturbations from the equilibrium state of thermal diffusion and thereafter the return to the equilibrium state on removal of the stress are more usefully considered in terms of the occurrence of events with the passage of time rather than in terms of the rate at which these events occur. This has led to a provocative suggestion that a sub-T_g relaxation is a precursor to the main or α-relaxation, which in turn leads ultimately to the viscous flow when the mechanical stress (or equivalently a large increase in electric polarization when an electric field) on a glassy solid is maintained for a substantially long period.[5] These theoretical descriptions have led to the prediction that viscous flow of a glass is possible only when localized motion in it has occurred. Alternatively stated, all glassy materials should show sub-T_g relaxations.

The above given concepts can be put to critical tests by a variety of experiments among which those that require mechanical stress for perturbation are particularly valuable, because this stress couples with all modes of diffusion of a molecule or molecular segment, in contrast with the electrical stress which couples only with the modes of diffusion that reorients a dipole vector. It is generally recognized that, although like dielectric relaxation, mechanical relaxation studies be carried out under isothermal conditions, the lack of a suitable technique has made studies of the mechanical loss spectrum of polymeric glasses difficult, and a survey of the literature showed that virtually no studies of the isothermal frequency dependence of the mechanical modulus for the sub-T_g relaxations have so far been done. As part of our detailed investigations of sub-T_g relaxation processes in polymers and other glassy materials, we report a detailed and systematic study of the β-relaxation of poly(methyl methacrylate) of well-characterized molecular weight and interpret the results in terms of the various concepts of localized diffusion. We further develop a procedure for the analysis of the modulus data in terms of a relaxation time distribution function and show that the complex modulus follows this function but gives values of the asymmetric distribution parameter and the strength of the relaxation whose meanings are not clear. We then reanalyze the results by a new formula for distribution which also produces an asymmetric spectrum and provides meaningful values of the distribution in terms of both the activation enthalpy and activation entropy for the β-relaxation process. It allows us to numerically simulate the fixed-frequency data of the complex shear modulus measured with varying temperature. In addition to the importance of these data for the understanding of molecular dynamics in polymers, we hope that the results will provide an incentive for both further and detailed studies of sub-T_g mechanical relaxations in amorphous polymers and their accurate theoretical analysis.

II. Experimental Methods

Samples of poly(methyl methacrylate) (PMMA) were obtained from NORSOLOR, France, who prepared and characterized it. Its molecular weight is 70 000 and its polydispersity index is 1.8. The samples, which were compression molded, were cut into bars of nominal dimensions 40 × 5 × 2.3 mm, two holes were drilled at each end of the bar, and each sample was mounted inside an

---

[†] McMaster University.
[‡] Institut National des Sciences Appliquées.

0024-9297/91/2224-4713$02.50/0

inverted forced torsional oscillation pendulum manufactured by Metravib S.A., France. The lower end of the sample is held fixed and the upper end is subjected to forced torsional oscillation of a desired frequency through a set of Helmholtz coils. The geometry of the sample was in accordance with the conditions that allow domination of shear as the deformation under a torsional stress. The relative deformation of the sample during the measurement was maintained at less than 10^{-4}.

The temperature of the sample was controlled by means of a furnace that surrounded it. The assembly was hermetically sealed within a stainless steel shroud which was immersed in liquid nitrogen contained in a Dewar flask. Such an assembly allowed isothermal measurements below 298 K during the 8 h required for the data collection. During the course of the measurement, the temperature increased by about 1.5 K, particularly during the 3-h period of data collection at a frequency of 2×10^{-4} Hz. In the hermetically sealed condition, the sample was maintained in an environment of about 0.5-atm pressure of argon gas. This provided an inert environment and prevented ice formation on the surface of the sample.

The real and imaginary components of the complex shear modulus G^* ($=G' + iG''$) and tan ϕ ($=G''/G'$) were measured over a frequency range 2×10^{-4} to 1 Hz for each of the temperatures at which the PMMA sample was isothermally kept. In our procedure, isothermal measurements were first carried out at low temperatures and thereafter the isothermal spectra were measured at predetermined temperature intervals by increasing the sample's temperature in steps. G^* and tan ϕ of several samples were also measured over a temperature range 100–400 K at fixed frequencies of 0.1 and 1.0 Hz. Residual stresses, if present, were removed on thermal cycling and were not observed to affect the β-relaxation strength in our samples of this study.

The glass transition temperature of the PMMA was measured at a heating rate of 10 K/min by means of a DSC 4 Perkin-Elmer differential scanning calorimeter. Determined from the onset point of the endotherm its value is 375 K. All PMMA samples were studied in their as-received state, and no effort was made to determine their water content.

III. Results

The isothermal spectra of the real and imaginary components, G' and G'', respectively, of the complex shear modulus G^* and the loss factor tan ϕ ($=G''/G'$) were obtained for the "as-received" sample in the temperature range 200–300 K. Among these spectra only those which were measured at temperatures between 230 and 270 K showed a peak in G'' and tan ϕ over the frequency range of our measurements. Typical spectra of G' and G'' and tan ϕ obtained at different temperatures are shown in Figures 1 and 2, respectively. The figures show that as the temperature increases, G' decreases and its spectrum shifts toward the high-frequency side. Both G'' and tan ϕ exhibit a peak whose position also shifts toward the high-frequency side and whose height increases as the temperature increases. This increase in height means that a horizontal shift along the frequency plane alone would not allow a superposition of the G', G'', and tan ϕ data and therefore the time–temperature superposition of the spectra cannot be satisfactorily made. Figures 1b and 2 also show that the shape of the spectrum is asymmetric with greater broadness on the high-frequency than on the low-frequency side. This is clearly evident from the dashed line drawn for an assumed symmetric shape of the spectra measured at 239 K which does not follow the data points in Figure 1b.

The frequency at which G'' reaches a maximum value of f_m at the different temperatures of measurements is plotted logarithmically against the reciprocal temperature in Figure 3. The data for the frequency at which tan ϕ reaches a maximum value are also included in Figure 3, as well as the two data points obtained from the measurements at fixed frequencies of 0.1 and 1 Hz. The frequency of maximum G'', or f_m, in Figure 3 varies according to the Arrhenius equation, $f_m = f_0 \exp(-E/RT)$ with $f_0 = 609$ THz and $E = 77.8$ kJ/mol. The corresponding plot of f_m when tan ϕ reaches a maximum value is also shown in Figure 3. This plot also follows the Arrhenius equation with $f_0 = 200$ THz and $E = 77.8$ kJ/mol.

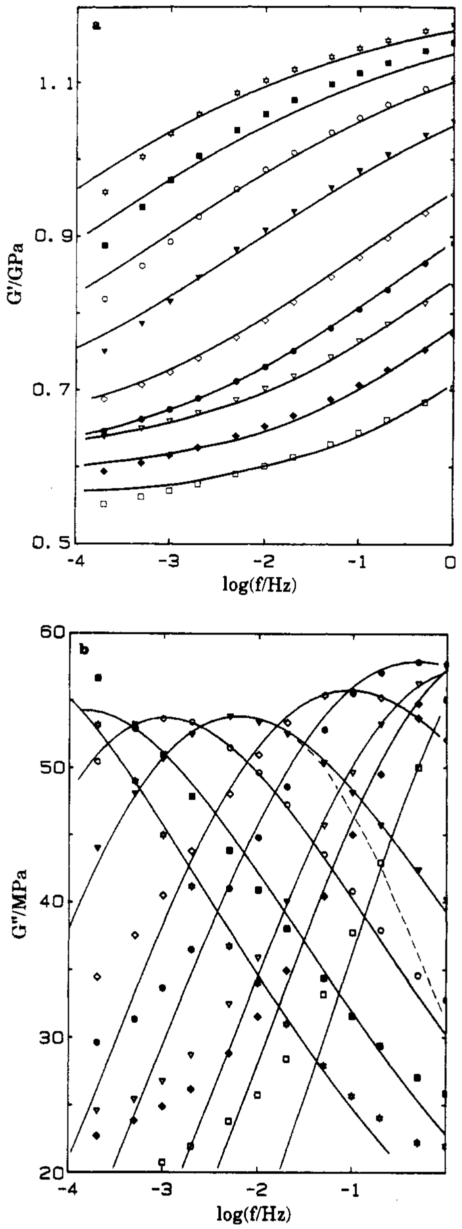

Figure 1. Isothermal spectra of G' (a) and G'' (b) for the β-relaxation process in poly(methyl methacrylate) at several temperatures. The continuous line is calculated for a stretched exponential relaxation function with parameters given in Table I. The notations for the temperatures are (✡) 207, (■) 218, (○) 229, (▼) 239, (◇) 256, (●) 269, (▽) 276, (◆) 289, and (□) 300 K.

IV. Discussion

Since the analysis of the relaxation data obtained here is being done in the G' and G'' rather than the tan ϕ formalism, it is important to determine first what effects our neglect of the changes in the sample's dimensions with change in temperature has on the measured G' and G'' values. While it is obvious that the value of tan ϕ of a material is independent of the errors in the measurements of the size and changes in the geometry of the sample under study, the values of G' and G'' are sensitive to such errors as well as to the changes in the sample's dimensions with changing temperature. This is particularly so in our study which requires for the calculation of G^* the

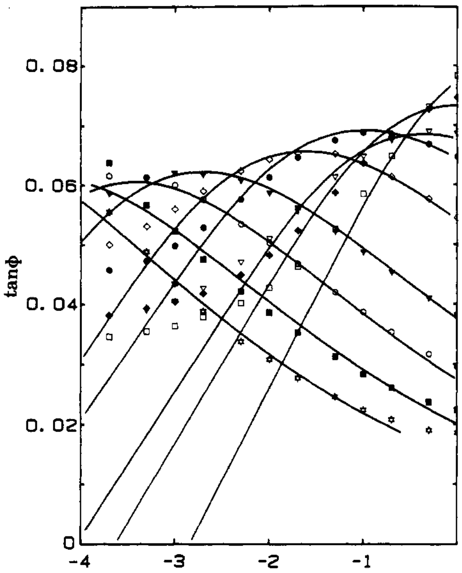

Figure 2. Isothermal spectra of tan ϕ for the β-relaxation process in poly(methyl methacrylate) at several temperatures as for Figure 1. The continuous line is calculated by a procedure as explained in the text with parameters given in Table I.

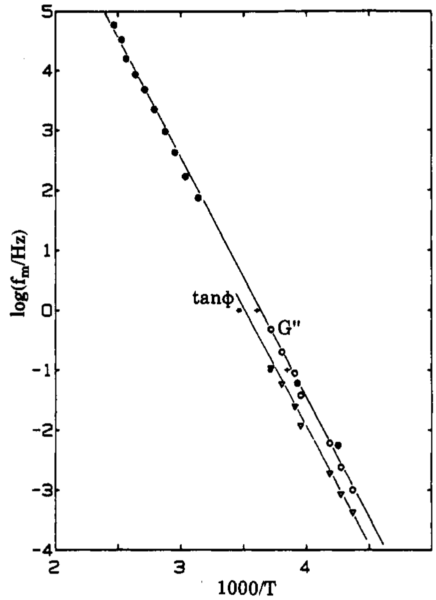

Figure 3. Frequency of the isothermal maximum of G'' and tan ϕ for the β-relaxation process in poly(methyl methacrylate) plotted against the reciprocal temperature. Data for the plots were obtained from (▽) tan ϕ isothermal peaks, (*) tan ϕ isochronal peaks, (○) G'' isothermal peaks, and (+) G'' isochronal peaks. Also included are the data (shown by dots) interpolated from the dielectric measurements of ϵ'' in ref 25.

knowledge of the shape factor calculated from the dimensions of the sample, and this shape factor increases with the dimensions of the sample. If the shape factor is less than the true value, the calculated G' and G'' are greater than the true values. Therefore, in measurements made with changing temperature, the changes in G' and G'' calculated from the data represent an algebraic sum of (i) a change that is intrinsic to a material and (ii) a change caused by the contraction or expansion of the sample, which is usually overlooked. In isochronal or fixed-frequency measurements, the dimensions of a sample under study are usually determined at room temperature, and these dimensions decrease on cooling and increase on heating it. If no corrections for these changes are made, the measured values of G' and G'' are lower than the true values when the sample has contracted on cooling and greater than the true values when the sample has expanded on heating. In our study the dimensions of the sample were measured at ~298 K; the lowest temperature of measurement may be as low as 100 K and as high as 350 K. The volumetric coefficient of thermal expansion of PMMA at temperatures below T_g is about 2×10^{-4} K^{-1}.[6] Therefore the calculated decrease in the linear dimensions of the sample from 298 to 100 K is 1.4% and the calculated increase from 298 to 350 K is 0.3%. These correspond to a 4% underestimate of the values of G' and G'' at the lowest temperature and a 1% overestimate at the highest temperature of the true values. In the temperature range 200–300 K, where our spectra were measured, the underestimate of G' and G'' is at most 2.4%, which is greater than our experimental error. Nevertheless, these errors are monotonic functions of temperature and they decrease as the temperature of the measurement approaches 298 K. However, values of the shear modulus of PMMA reported here should be considered as indicative of the relative changes of G' and G'' with frequency. Therefore, a calibration of the apparatus should be made in order to obtain absolute values; under these conditions values of moduli given here have to be multiplied by a calibration factor, which is between 1.8 and 2. Within these restrictions, the analysis of the spectra still yields valuable information on the molecular processes of PMMA, which are discussed as follows.

1. Shape of the G^* Spectrum. One of the main difficulties in the description of the mechanical spectrum is the lack of availability of data over a wide enough frequency range, which would allow an unambiguous determination of the relaxation function. Nevertheless, the variety of relaxation functions[7,8] that are used to study the mechanical relaxation require description of the shear modulus, G^*, by

$$G^*(i\omega\tau) = G'(\omega\tau) + iG''(\omega\tau) \tag{1a}$$

where

$$G'(\omega\tau) = G_R + (G_U - G_R) \int_{-\infty}^{+\infty} \psi(\ln \tau) \frac{\omega^2\tau^2}{1 + \omega^2\tau^2} \, d(\ln \tau) \tag{1b}$$

and

$$G''(\omega\tau) = (G_U - G_R) \int_{-\infty}^{+\infty} \psi(\ln \tau) \frac{\omega\tau}{1 + \omega^2\tau^2} \, d(\ln \tau) \tag{1c}$$

where G' and G'' are the real and imaginary components of the shear modulus, G_U and G_R are the unrelaxed and relaxed moduli, ω is the angular frequency, τ is the relaxation time, and ψ is the relaxation time distribution function. The relaxation time distribution function can be obtained by fitting the data to eq 1b and 1c, but it requires inversion of integrals of a response function,[7,8] which in turn can only be done approximately. An indirect and simpler method that is often used involves a spectral distribution function with an empirical parameter known as a distribution parameter. When the distribution of relaxation time varies with temperature, the first method of determining $\psi(\ln \tau)$ yields more information than the second or indirect method, for it allows one to express $\psi(\ln \tau)$ in terms of both a distribution of activation entropies and a distribution of enthalpies and thereby helps us to understand the physical origin of the relaxation process. With the above-mentioned considerations in mind, we discuss the shape of the β-relaxation spectra as follows:

(i) Description by the Kohlrausch–Williams–Watts (KWW) Equation and the Temperature Dependence of the Relaxation Parameter. In Figure 1, the isothermal spectra of G' and G'' are seen to be asymmetric, and the shape of the G'' peaks resembles that which is described by a stretched exponential, or Kohlrausch–Williams–Watts[9,10] empirical, relaxation function. Therefore, we analyze both the G' and G'' spectra of Figure 1 according to a functional form

$$\phi(t) = \phi_0 \exp(-[(t/\tau_0)^{\beta}]) \qquad (2)$$

where $\phi(t)$ represents a quantity whose value decreases with time t, ϕ_0 is the initial value of the quantity, τ_0 is a characteristic relaxation time, and β is an empirical parameter of value between zero and one. When $\beta = 1$, the G'' spectrum is Debye-like with a half-width of 1.144 decades and when $\beta = 0$, the half-width of the spectra is formally infinite. For values of $\beta < 1$, the function of eq 2 is known as the Kohlrausch[9,10]–Williams–Watts[11–13] function, which has been a subject of both mathematical modeling[14–16] and physical significance in recent years.[17,18]

Montroll and Bendler[15] and Dishon et al.[19] have described analytical procedures for the analysis of dielectric relaxation data according to eq 2. Since the procedure for calculation of G^* differs from that for the dielectric permittivity, we modify the equations and the analytical procedure given by Dishon et al.[19] and further develop them for our purpose here as follows:

From eqs 1a and 2

$$\frac{G_U - G'(\omega)}{G_U - G_R} + i\frac{G''(\omega)}{G_U - G_R} = -\int_0^{\infty} e^{-i\omega t}\left(\frac{d\phi(t)}{dt}\right) dt \qquad (3)$$

where G' and G'' are the real and imaginary components of the shear modulus, G_U is the unrelaxed modulus (or high-frequency modulus), G_R is the corresponding relaxed modulus (or low-frequency modulus), and $\phi(t)$ has the functional form given by eq 2. $(G_U - G_R)$, also written as ΔG, is the strength of the relaxation. Equations 2 and 3 together imply that for $z = \omega\tau$ and

$$\frac{G'(\omega) - G_U}{G_U - G_R} = \pi z V_{\beta}(z) - 1 \qquad (4)$$

and

$$\frac{G''(\omega)}{G_U - G_R} = \pi z Q_{\beta}(z) \qquad (5)$$

where V_β and Q_β are standard integrals given by

$$Q_{\beta}(z) = \frac{1}{\pi}\int_0^{\infty} \exp(-u^{\beta}) \cos(zu)\, du \qquad (6a)$$

$$= \frac{\beta}{\pi z}\int_0^{\infty} \frac{\exp(-u^{\beta})}{u^{1-\beta}} \sin(zu)\, du \qquad (6b)$$

$$V_{\beta}(z) = \frac{1}{\pi}\int_0^{\infty} \exp(-u^{\beta}) \sin(zu)\, du \qquad (7a)$$

$$= \left[1 - \int_0^{\infty} \frac{\beta}{u^{1-\beta}} \exp(-u^{\beta}) \cos(zu)\, du\right] \Big/ \pi z \qquad (7b)$$

The functions Q_β and V_β have been carefully evaluated by Dishon et al.[19] and tabulated for values of β from 0.01 to 2.0 as a function of z. When the functions for a desired value of β were not available in Dishon et al.'s tables,[19] we first linearly interpolated the numerical values of $V_\beta(z)$ and $Q_\beta(z)$ from the nearest values of β available in the tables. This interpolation caused unacceptably large errors in the values of β, as our detailed examination prior to using the interpolation procedure showed that $Q_\beta(z)$ and $V_\beta(z)$ are not monotonic functions of β, even for small changes in β. In fact $Q_\beta(z)$ reaches a peak value for certain values of β. Therefore for $0.1 < \beta < 0.2$, $Q_\beta(z)$ and $V_\beta(z)$ were numerically evaluated from eqs 6b and 7b, instead of from eqs 6a and 7a, as they allowed a relatively more rapid convergence of values, and the calculated values were cross-checked against those given by Dishon et al.[19] In our procedure here, we first constructed plots of $[\pi z V_\beta(z) - 1]$ and $\pi z Q_\beta(z)$ against $\log(z/z_m)$ for $\beta = 0.10$–0.20, which are shown in Figures 4 and 5, respectively.

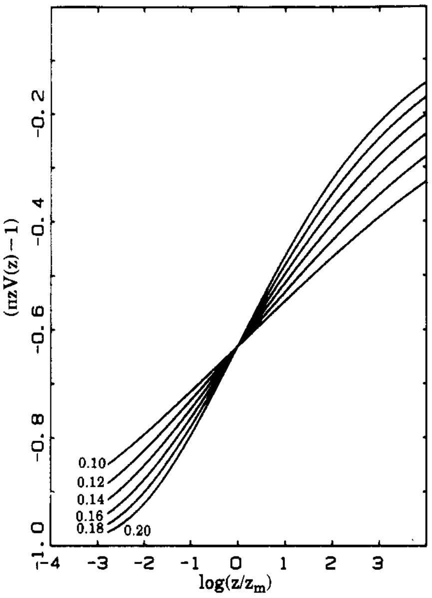

Figure 4. Universal curves of $[\pi z V_\beta(z) - 1]$ for a stretched exponential relaxation function calculated for several values of β plotted against $\log(z/z_m)$. Numbers next to the curves refer to the value of β. Values of z_m correspond to the maxima of $\pi z Q_\beta(z)$ curves and are equal to 0.6 Hz when $0.10 \le \beta \le 0.20$.

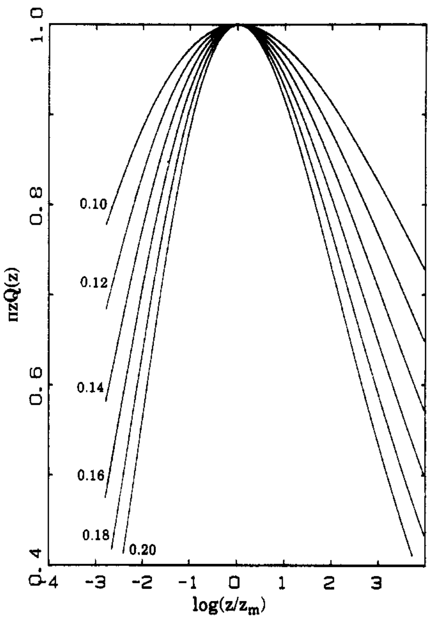

Figure 5. Universal curves of $\pi z Q_\beta(z)$ for a stretched exponential relaxation function for several values of β plotted against $\log(z/z_m)$. Numbers next to the curves refer to the value of β. Values of z_m correspond to the maxima of $\pi z Q_\beta(z)$ curves and are equal to 0.6 Hz when $0.10 \le \beta \le 0.20$.

In Figure 4, the values of $[\pi z V_\beta(z) - 1]$ are plotted against $\log(z/z_m)$ in the range from -1, when $z = 0$, to 0, when $z \to \infty$. In this figure, the spread of the plots becomes progressively less and the maximum slope of the plots that appears at $(z/z_m) = 1$ becomes progressively greater as $\beta \to 1$. The corresponding plots of $\pi z Q_\beta(z)$ seen in Figure 5 show a peak that occurs at $(z/z_m) = 1$ with a half-width that decreases as $\beta \to 1$ and a shape of the peak that becomes increasingly stretched at values of $z > z_m$ as $\beta \rightarrow 0$. The change in the shape of both $[\pi z V_\beta(z) - 1]$ and $\pi z Q_\beta(z)$ plots is of course as expected from eqs 2 and 3 and as implied in the calculation of Montroll and Bendler[15] and Dishon et al.[19]

The plots in Figures 4 and 5 are particularly valuable for determining the parameters of the KWW or stretched exponential relaxation function when data of G' and G'' are limited to a narrow frequency range, as is usually the case, but are sufficient to allow the construction of normalized plots of G''. We use the values from the tables[19] to determine the shape of the mechanical spectra seen in Figures 1 and 2 as follows:

In our procedure, first the curves of $[\pi z V_\beta(z) - 1]$ and $\pi z Q_\beta(z)$ against log f were horizontally shifted so that the maximum of $\pi z Q_\beta(z)$ corresponds to the frequency f_m of the maximum of G'' (f_m either given by the experimental data or extrapolated from the Arrhenius plot when G''_{max} was not observed). The numerical value of this displacement in turn is equal to log $(2\pi\tau_0/z_m)$, where z_m is the value of z when $\pi z Q_\beta(z)$ reaches a maximum in Figure 5. Since the value of z_m is already known, τ_0 of eq 2 could be calculated. This τ_0 differs from the τ_m obtained from the frequency f_m when $G'' = G''_{max}$ and is related to the average relaxation time $\langle\tau\rangle$ by the equation[13]

$$\langle \tau \rangle = \frac{\tau_0}{\beta}\Gamma\left(\frac{1}{\beta}\right) \qquad (8)$$

where Γ denotes the gamma function.

Then we use eqs 4 and 5 and the tables of $[\pi z V_\beta(z) - 1]$ and $\pi z Q_\beta(z)$ to calculate the spectra of G'' and G' for various values of β, G_R, and G_U until the calculated curves match the experimental data in both G' and G''. This provided us a value of β within an accuracy of ±0.01. (The procedure we used thus avoided simultaneous nonlinear regression necessary for such data fitting and yet allowed determination of β, G_U, and G_R with sufficient accuracy.)

Finally, we combine eqs 4 and 5 and calculate the value of tan ϕ from

$$\tan\phi = \frac{G''}{G'} = \frac{\pi z Q_\beta(z)}{(G_U/\Delta G) + [\pi z V_\beta(z) - 1]} \qquad (9)$$

Since G_U and G_R depend on a material's chemical and physical constitution, universal curves of tan ϕ against z/z_m similar to those of G' and G'' cannot be obtained. Therefore, tan ϕ values for each isothermal experiment were calculated by using individual values of β, G_R, and G_U and they superposed the tan ϕ data as seen in Figure 2.

In Figure 1b, the measured values of G'' at the lowest frequencies on the low-frequency side of the spectrum are higher than the calculated values of G''. This is caused by a contribution to G'' from the α-relaxation process which is greater at the lowest frequency of our measurements. Furthermore, the contribution from the α-relaxation process is generally anticipated to be higher at a higher temperature as the β- and the α-relaxation peaks tend to merge[8,20] with increasing temperature. But, since the G'' peaks for the α- and β-relaxation processes for PMMA here, as for other polymers, have comparable heights and since this height is known to decrease with increasing temperature for the α-process and to increase with increasing temperature for the β-process, the increase in the temperature may decrease the relative magnitude of the contribution from the α-process. This suggests that the net effect on measured G'' at the lowest frequencies of the β-relaxation or the highest frequency of the α-relaxation spectrum would be a partial or complete compensation of the change with temperature of the G'' contributions from the two relaxations. It seems therefore that the deviations of the measured G'' (in Figure 1b) from the calculated values, as found here, may not progressively increase with increase in the temperature of measurement of the β-relaxation spectra. Nevertheless, since the tan ϕ peak for the α-relaxation process is nearly 2 orders of magnitude higher than that for the β-relaxation process, the deviations of the measured tan ϕ (in Figure 2) from the calculated values are expected to progressively increase with increasing temperature, as is found here, despite the fact that the height of the α-peak for tan ϕ decreases with increasing temperature and that of the β-peak for tan ϕ increases with increasing temperature.

For the low-temperature isothermal spectra, the measured G'' is higher than the calculated G'' on the high-frequency side as is seen in Figure 1b. This may be due to the proximity of an extra peak from the absorbed water in PMMA,[8] as no precautions were taken to remove water from PMMA before the experiment. Our studies have also shown that an increase in the water content raises the G'' and tan ϕ and lowers the G' for the β-relaxation process. In this study a comparison of the β-relaxation spectra is still justified as all isothermal spectra were measured for the same sample with no modification of the water content, if any.

We now discuss the uncertainty in the various parameters obtained by using our procedure, rather than the nonlinear regression analysis, and their effects on the fit of the data to eq 2. The frequency range of our isothermal experiments allows us to compare against the calculated curves only a small part of the peak in G'' and tan ϕ spectra, which corresponds to the near middle part of the G' spectra. In Figure 1a the continuous lines correspond to the previously defined horizontally shifted curve of $\Delta G[\pi z V_\beta(z) - 1] + G_U$ against log (f) and in Figure 1b to those of $\Delta G[\pi z Q_\beta(z)]$ against log (f), with values of ΔG, G_U, and β given in Table I. Similarly, continuous lines of the tan ϕ spectra in Figure 2 represent the previously defined horizontally shifted curves of $[\pi z Q_\beta(z)]/[(G_U/\Delta G) + [\pi z V_\beta(z) - 1]]$ against log (z). Since the fit of the G'' data is affected only by errors in ΔG and that of the G' and tan ϕ is affected by errors in both ΔG and G_U, the fit of the G'' data to the stretched exponential relaxation function seems more reliable than the fit of the G' and tan ϕ data.

As seen in Table I, the temperature dependence of the parameter β does not follow a trend. Furthermore, G_U increases with increasing temperature, which seems inconsistent with the general notion of change in phonon modes with temperature. It therefore seems that the analysis in terms of a stretched exponential relaxation function does not provide a physical insight for localized motions and further leads to observations generally inconsistent with the notions of the temperature dependence of the modulus. We note that although the stretched exponential function of eq 2 can be formally expressed in terms of a distribution of activation energies, as Bendler and Schlesinger[20] have shown, no procedure for determining these quantities has yet been developed.

(ii) Description by an Alternative Asymmetric Relaxation Time Distribution Function and the Temperature Dependence of Relaxation Parameters. As pointed out in section IV.1, it is more meaningful to describe the shape of the β-relaxation spectra in terms of a distribution of relaxation times for which the relaxation occurs in parallel rather than in series as the mechanism of such relaxations is unlikely to involve cooperativity or hierarchy of constrained motions. We therefore describe the shape of the β-relaxation spectra by an alternative relaxation time distribution function, based upon the

Gaussian function

$$\Psi\,[\ln(\tau/\tau_m)] = \frac{1}{B\pi^{1/2}}\exp\left(-\left[\frac{\ln(\tau/\tau_m)}{B}\right]^2\right) \qquad (10a)$$

where B is a parameter that is a measure of the width of a Gaussian distribution and τ_m is the most probable value of τ which corresponds to f_m, the frequency at the maximum in the G'' spectrum. The Gaussian distribution of eq 10a can be modified for our purpose to obtain an asymmetric spectra by introducing a parameter α, which is much less than unity, such that when $\tau < \tau_m$

$$\Psi_1'[\ln(\tau/\tau_m)] = \frac{1}{B\pi^{1/2}}\exp\left(-\left[\frac{\ln(\tau/\tau_m)}{B(1+\alpha)}\right]^2\right) \qquad (10b)$$

and when $\tau > \tau_m$

$$\Psi_2'[\ln(\tau/\tau_m)] = \frac{1}{B\pi^{1/2}}\exp\left(-\left[\frac{\ln(\tau/\tau_m)}{B(1-\alpha)}\right]^2\right) \qquad (10c)$$

Thus α, the asymmetry factor, makes the distribution broader for $\tau < \tau_m$ than for $\tau > \tau_m$. When $\alpha \ll 0$ (its value used here is 0.07), the magnitude of B can be used as an approximate measure of the distribution of activation energies and attempt frequencies, f_0. It should be noted that since the functions in eqs 10b and 10c are defined such that they are *not* normalized, the complex modulus must be written in the forms

$$\frac{G'(\omega) - G_R}{G_U - G_R} = \frac{\sum_\tau\left[\frac{(\omega\tau)^2}{1+(\omega\tau)^2}\exp\{-[\ln(\tau/\tau_m)/B(1+\epsilon\alpha)]^2\}\,\Delta\ln\tau\right]}{\sum_\tau[\exp\{-[\ln(\tau/\tau_m)/B(1+\epsilon\alpha)]^2\}\,\Delta\ln\tau]} \qquad (11)$$

and

$$\frac{G''(\omega)}{G_U - G_R} = \frac{\sum_\tau\left[\frac{\omega\tau}{1+(\omega\tau)^2}\exp\{-[\ln(\tau/\tau_m)/B(1+\epsilon\alpha)]^2\}\,\Delta\ln\tau\right]}{\sum_\tau[\exp\{-[\ln(\tau/\tau_m)/B(1+\epsilon\alpha)]^2\}\,\Delta\ln\tau]} \qquad (12)$$

where $\epsilon = +1$ for $\tau < \tau_m$ and $\epsilon = -1$ for $\tau > \tau_m$.

A change in the value of B with change in temperature for a fixed value of $\alpha \ll 1$ thus represents the change in the width of distribution in $\ln\tau$ with temperature, which for an Arrhenius temperature dependence, namely, $\tau = \tau_0 \exp[E/RT]$, means that the distribution arises from a distribution in $\ln\tau_0$ and/or E.

As discussed by Nowick and Berry,[7] if $\ln\tau_0$ and E are independent of each other, B is given by

$$B = [B_0^2 + (B_U/RT)^2]^{1/2} \qquad (13a)$$

where B_0 is a dimensionless quantity representing the width of the distribution in the temperature-independent parameter, $\ln\tau_0$, and B_U has the dimensions of energy and represents the width of distribution in E. However, when both $\ln\tau_0$ and E vary linearly with a single parameter, which may be a property of a material

$$B = B_0 + B_U/RT \qquad (13b)$$

Table I
Parameters of the Stretched Exponential Relaxation Function for the Dynamic Mechanical Spectra of the β-Relaxation Process in PMMA Measured at Different Temperatures

T/K	f_m/Hz	β	ΔG/GPa	G_R/GPa	G_U/GPa	$\langle\tau\rangle$/s
207	1.5×10^{-5} [a]	0.19	0.54	0.69	1.23	1.2×10^6
213	5.2×10^{-5} [a]	0.20	0.49	0.74	1.23	2.2×10^5
218	1.4×10^{-4} [a]	0.19	0.50	0.72	1.23	1.3×10^5
223	3.6×10^{-4} [a]	0.19	0.50	0.72	1.22	5.0×10^4
229	1.0×10^{-3}	0.19	0.50	0.72	1.22	1.8×10^4
234	2.4×10^{-3}	0.19	0.49	0.71	1.21	7.5×10^3
239	6.0×10^{-3}	0.18	0.52	0.69	1.21	5.1×10^3
253	3.8×10^{-2}	0.17	0.57	0.66	1.23	1.5×10^3
256	8.9×10^{-2}	0.17	0.57	0.66	1.23	6.2×10^2
263	2.0×10^{-1}	0.16	0.62	0.64	1.25	5.5×10^2
269	4.8×10^{-1}	0.16	0.63	0.63	1.26	2.3×10^2
271	1.0[a]	0.16	0.63	0.65	1.27	1.1×10^2
276	1.7[a]	0.17	0.59	0.64	1.23	3.3×10^1
284	2.6[a]	0.17	0.61	0.63	1.24	2.1×10^1
289	4.3[a]	0.17	0.61	0.61	1.21	1.3×10^1
294	8.5[a]	0.17	0.63	0.60	1.23	6.5
300	16[a]	0.18	0.62	0.59	1.21	1.9

[a] Frequencies deduced from the Arrhenius plot of the isothermal maximum of G'' seen in Figure 3.

We now use eqs 11 and 12 to fit the data of Figure 1 with essentially the same normalization and curve-shifting procedures as for fitting the data to the KWW function. These fits are shown in Figure 6. For the spectra at temperatures 207, 213, 218, 223, 271, 276, 284, 289, 294, and 300 K, where the G''_{max} or G'' peak is not observed, f_m was determined from an extrapolation of the Arrhenius plots in Figure 3. The experimental data and the calculated spectra for G' and G'' at different temperatures are also shown in Figure 6, and those for tan ϕ in Figure 7. It is evident that the data are adequately described by the new relaxation time distribution of eqs 10b and 10c, with the various parameters given in Table II. These parameters are plotted against the temperatures in Figures 8 and 9.

The plots in Figures 8 and 9 reveal an important difference between the conclusions derived from the fit of the data to the KWW function and that from the fit to the relaxation time distribution function of eqs 10b and 10c as follows: First, the latter function leads to a more realistic temperature dependence of G_U, ΔG, and B than does the former function in that (a) G_U decreases with increasing temperature at a rate of $((1/G_U)\partial G_U(\partial T) \approx 0.001$, which is consistent with the temperature dependence of the elastic modulus anticipated from phonon interactions, (b) the relaxation strength increases with increasing temperature according to an approximate equation $\Delta G(T) = 4.33 \times 10^8 + 3.54 \times 10^5 T$, which implies that G_R decreases with increasing temperature, and (c) a decrease in G_R with increase in temperature is directly observable, which means that ΔG for the α-relaxation process decreases with increasing temperature, since G_R(β-process) = G_U(α-process) and G_R(α-process) is 3 orders of magnitude lower than the G_U(α-process).

One of the important aspects of this analysis of the shape of the β-relaxation spectra, as mentioned earlier here, is that the value of B in eqs 10b and 10c has a physical significance in terms of the distribution of activation energies, which can now be examined. Equations 13a and 13b are interpreted in terms of the variations of both E and $\ln\tau_0$, under conditions when E and $\ln\tau_0$ are either interdependent or independent of each other. As a first approximation, we consider the former for which Figure

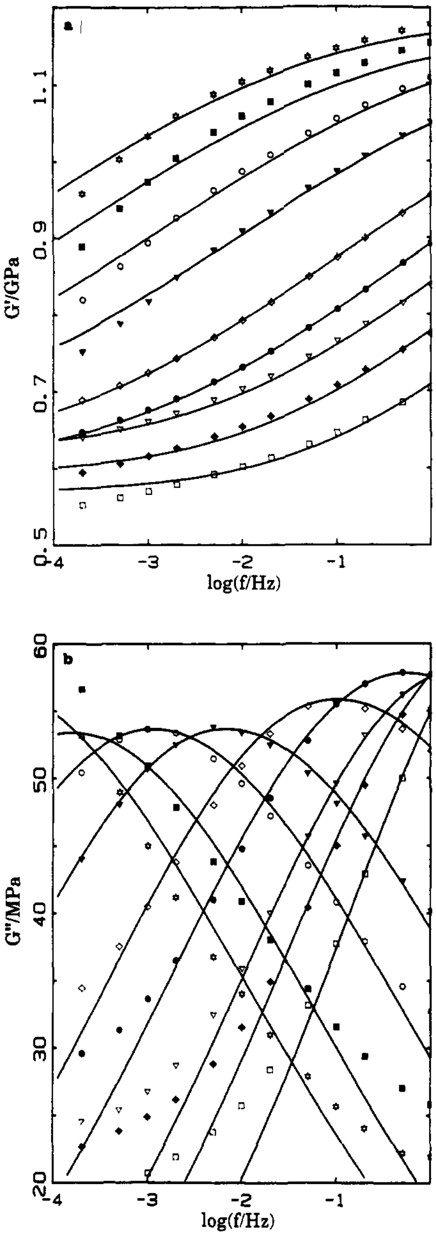

Figure 6. Isothermal spectra of G' (a) and G'' (b) for the β-relaxation process in poly(methyl methacrylate) at several temperatures. The continuous line is calculated from the new relaxation time distribution function with parameters given in Table II. The notations are the same as in Figure 1.

9 shows that the variation of B with temperature obtained by linear regression procedure is given by $B = 6.143 + 424.2T^{-1}$, which gives $B_0 \approx 6 \pm 1$ and $B_U = 3.5 \pm 0.6$ kJ/mol. Accordingly, the distribution of relaxation times for the β-relaxation process indicates a distribution of both the preexponential factor τ_0 and E. The energy of activation is 77.8 kJ/mol with a distribution width of 3.5 kJ/mol, and $\ln \tau_0$ is -36 with a distribution width of 6.

Finally, the self-consistency of the analysis in terms of a relaxation time distribution function of eqs 10a and 10b can be examined by calculating, from eqs 1b and 1c and eqs 10a and 10b using the parameters given in Table II and the values of E and τ_0 in the Arrhenius equation, the variation of G' and G'' with temperature for a fixed frequency of measurement. This variation expressed as $\tan \phi$ ($=G''/G'$) for two frequencies 0.1 and 1 Hz is shown in Figure 10, where the experimental data are included for comparison. The data were obtained for an as-received sample, which agreed with those measured as isothermal spectra. Evidently, the data are in reasonably good agreement with the calculated isochrones. We believe that this strongly indicates the usefulness of the new distribution function for the analysis of β-relaxation processes in poly(methyl methacrylate), and, on this basis, suggest

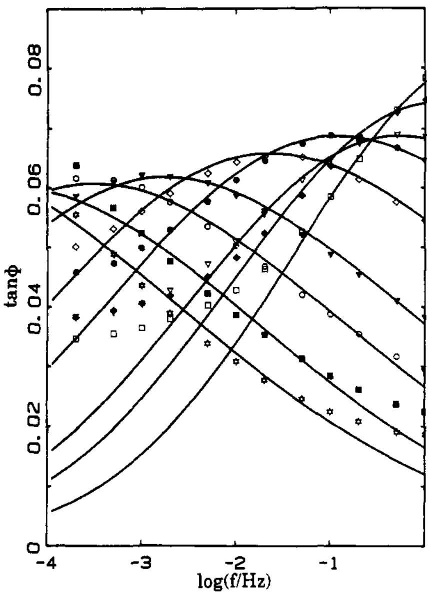

Figure 7. Isothermal spectra of $\tan \phi$ for the β-relaxation process in poly(methyl methacrylate) at several temperatures as for Figure 1. The continuous line is calculated by a procedure as explained in the text with parameters given in Table II.

Table II
Parameters of the Fit of the Data for Dynamic-Mechanical Spectra of the β-Relaxation in PMMA to a Modified Gaussian Distribution

T/K	f_m/Hz	B_{gauss}	ΔG/GPa	G_R/GPa	G_U/GPa
207	$1.5 \times 10^{-5\,a}$	8.5	0.57	0.63	1.19
213	$5.2 \times 10^{-5\,a}$	7.5	0.49	0.69	1.18
218	$1.4 \times 10^{-4\,a}$	7.8	0.49	0.68	1.17
223	$3.6 \times 10^{-4\,a}$	7.8	0.49	0.68	1.17
229	10^{-3}	8.0	0.50	0.67	1.17
234	2.4×10^{-3}	8.0	0.50	0.67	1.17
239	6.0×10^{-3}	8.1	0.50	0.63	1.16
253	3.8×10^{-2}	8.0	0.52	0.63	1.16
256	8.9×10^{-2}	8.3	0.54	0.62	1.16
263	2.0×10^{-1}	8.3	0.55	0.62	1.16
269	4.8×10^{-1}	8.3	0.56	0.60	1.16
271	1^{a}	8.0	0.54	0.63	1.18
276	1.7^{a}	7.5	0.51	0.62	1.14
284	2.6^{a}	7.5	0.52	0.62	1.14
289	4.3^{a}	7.3	0.52	0.59	1.11
294	8.5^{a}	7.3	0.54	0.58	1.13
300	16^{a}	7	0.54	0.57	1.11

[a] Frequencies deduced from the Arrhenius plot of the isothermal maximum of G'' seen in Figure 3.

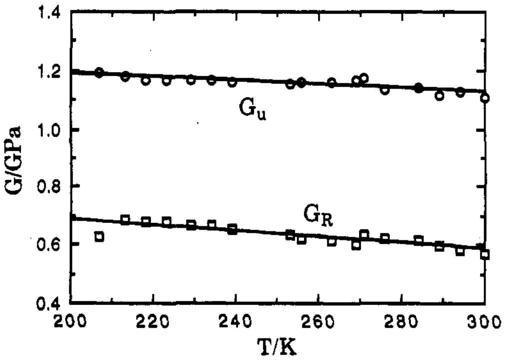

Figure 8. Magnitude of G_R (□) and G_U (○) for the β-relaxation process in poly(methyl methacrylate) plotted against the temperature. These data are obtained from the analysis using the new relaxation time distribution function with parameters given in Table II. The least-squares linear fitting gives G_U (Pa) = $13.20 \times 10^8 - 6.48 \times 10^5 T$ and G_R (Pa) = $8.87 \times 10^8 - 1.00 \times 10^6 T$.

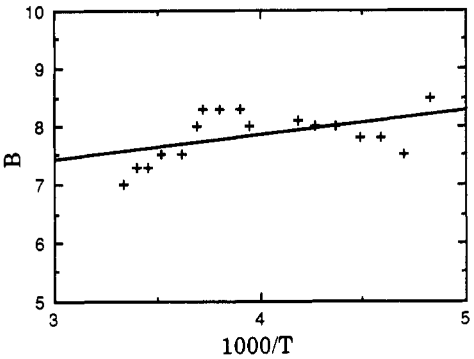

Figure 9. Temperature dependence of B, the parameter of the new relaxation time distribution function. B is plotted against the reciprocal temperature. The least-squares linear fitting gives $B = 6.143 + 424.2/T$.

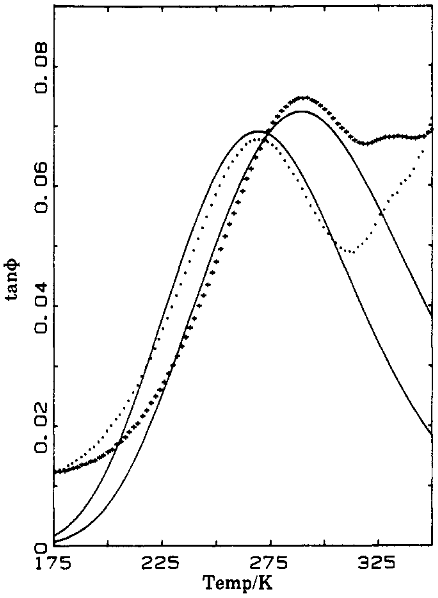

Figure 10. Measured isochrones of tan ϕ for the β-relaxation process in poly(methyl methacrylate) at 1 (+) and 0.1 Hz (•). The continuous line is calculated by using the temperature dependence of G_R, G_U, and B as shown in Figures 8 and 9.

its use in the future for other polymers and molecular glasses.

It should be noted that Havriliak and Negami's[21] empirical equation could also be useful for our analysis, for it too produces an asymmetric spectrum, but like the KWW function, the parameters obtained from the analysis do not seem to be readily interpretable in terms of a distribution of E and preexponential factors, information which is needed if physical insight into a relaxation phenomenon were to be achieved. In this sense we suggest that an analysis in terms of a relaxation time distribution of eqs 10a and 10b is preferable, as also pointed out by MacDonald.[22] The preceding analysis clearly demonstrates this.

Starkweather[23] has recently used a different procedure to conclude that the dielectric and mechanical spectra of β-relaxation processes in polycarbonate and PMMA may be regarded as a noncooperative process with a distribution of both the activation enthalpies and activation entropies. However, his procedure did not reveal a distribution of activation entropies for the β-relaxation process, although it did so for the α-relaxation process.

Now despite the limitations of the activated complex theory as an explanation for molecular diffusion phenomena, we use Starkweather's procedure[23] and determine the free energy (ΔF^*), the enthalpy (ΔH^*), and the entropy (ΔS^*) for the β-relaxation process in PMMA. According to Eyring's equation

$$f = (kT/2\pi h)\exp(-\Delta F^*/RT) = (kT/2\pi h)\exp(\Delta S^*/R)\exp(-\Delta H^*/RT) \quad (14)$$

a plot of ln (f_m/T) against the reciprocal temperature is a straight line with slope $-(\Delta H^*/R)$ and a high-temperature intercept [ln $(k/2\pi h) + (\Delta S^*/R)$]. From such a plot (not included here) we obtain ΔH^* of 76.3 kJ/mol and ΔS^* of 48.3 (J/mol)/K for β-relaxation in PMMA. This ΔH^* is comparable with 77.8 kJ/mol, the value of E of the Arrhenius equation as determined in the earlier section.

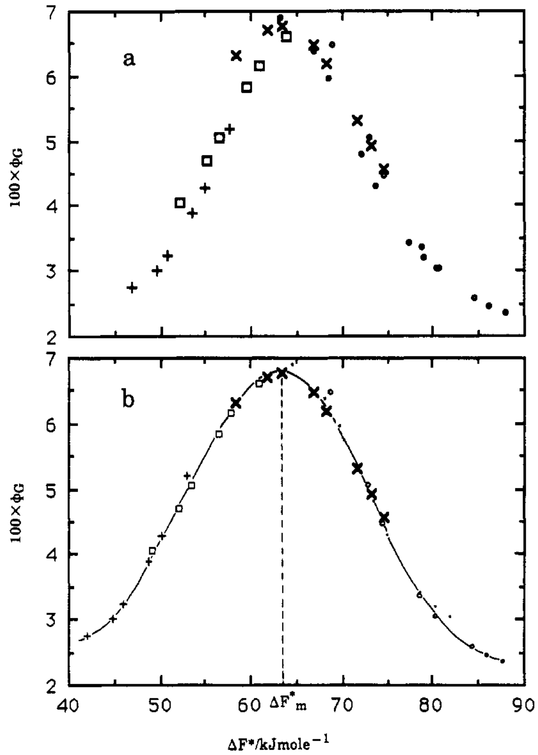

Figure 11. Distribution of the free energy of activation, ΔF^*, for the β-relaxation process in poly(methyl methacrylate): (a) at different temperatures; (b) shifted to meet the curve for 256 K. Notations for temperatures are (+) for 207 K, (□) for 229 K, (×) for 256 K, (●) for 276 K, and (○) for 300 K. The shift of the data in (b) can be obtained from a comparison against (a).

The ΔS^* of 48.3 (J/mol)/K, although much smaller than that observed by Starkweather[23] for the α-relaxation processes, is nevertheless significant, and its effect can be seen in the plots of distribution, ϕ_G, against ΔF^* to be similar to that in the corresponding plots for the α-relaxation process as follows: The ΔF^* can be calculated as a function of f and T from

$$\Delta F^* = RT[\ln(k/2\pi h) + \ln(T/f)] \quad (15)$$

and ϕ_G from [23]

$$\phi_G = 2G''(\omega)/\pi\Delta G \quad (16)$$

Plots of ϕ_G against ΔF^* for different temperatures are shown in Figure 11a. Here the data lie on different curves, which shift toward low values of ΔF^* with increase in the temperature. This shift is a reflection of the fact that ΔS^* for the β-relaxation process is significant. As in Starkweather's procedure,[23] the data can be horizontally shifted toward a reference temperature of 256 K to construct a single curve as seen in Figure 11b. The shape of this single curve is seen to be asymmetric and broader at low than at high values of ΔF^*, which indicates self-consistency of our analysis in terms of an asymmetric relaxation time distribution function.

The self-consistency of our analysis can be examined by one further procedure which involves calculation of ΔS^* from a combination of parameters used in the Eyring and Arrhenius equations, namely

$$T\Delta S^* = E - \Delta F^* - RT \qquad (17)$$

From the mean value of ΔF^* shown by the dashed line in Figure 11b and E = 77.8 kJ/mol, we obtain ΔS^* = 49.5 (J/mol)/K, which is comparable to ΔS^* = 48.3 (J/mol)/K obtained from the high-temperature intercept of the Eyring plot from eq 14. This agreement confirms that our estimate for ΔS^* for the β-relaxation process is reliable.

The value of ΔS^* also provides justification for the dependence of the parameter B on temperature shown in Figure 9, for if B (=7.8) was taken to be independent of temperature, the width of the distribution of ΔS^* would be ±65 (J/mol)/K, which is larger than the average value of 49 (J/mol)/K for ΔS^*. The data in Figure 9 also do not suggest that B would linearly approach zero as $T \rightarrow \infty$, although the possibility of a nonlinear approach to zero is not ruled out. This approach cannot be experimentally studied because the β- and α-relaxation processes merge as $T \rightarrow T_g$, making an unambiguous determination of the characteristics of the β-relaxation spectrum difficult. In fact, the value proposed for the distribution of ln τ_0 ($B_0 \approx 6$) yields through eq 14 a value of ΔS^* distributed from 0 to 100 (J/mol)/K (with an average value of 50 (J/mol)/K).

Stretched exponential and symmetric Gaussian distribution functions have been used by Wehrle et al.[24] and Rössler[25] to fit their data, and the similarity and differences between the two functions in the short-time range have been discussed by Wehrle et al.[24] Our analysis here of course differs from theirs, and despite the formal requirement for negative activation energies implied in a Gaussian distribution, albeit with a relatively small contribution to the integrals, and the use of three parameters in eqs 10b and 10c instead of two in the KWW equation, we believe that the information regarding the β-relaxation spectra deduced here justifies the use of the distribution expressed by eqs 10b and 10c. Procedures for obtaining similar information from fitting the data to the KWW equation, when available, would of course provide, through a new set of parameters, a further stimulus for such studies.

Because of a substantially large width of the distribution of free activation energies for the β-relaxation, one is faced with a greater challenge in seeking an unambiguous formalism for the shape of the β-relaxation spectrum and if, as in an earlier theory,[5] β-relaxation is precursor of the α-relaxation, its spectral shape may play an important role in the understanding of the evolution of the α-relaxation spectrum.

2. The Frequency-Independent Background Loss. In all mechanical measurements by flexure, extension, or torsional oscillations, the measured tan ϕ contains a contribution from the mechanical properties of the materials used as clamps or suspensions fibers, although the contributions are often negligibly small.[26] In addition, it is often considered[27,28] that materials possess a background loss that is frequency independent and that contributes only to G'' but not to G'. This loss is found to be temperature dependent,[27] and attempts have been made to arbitrarily fit this background loss to different equations by considering that the value of tan ϕ at the minima in the isochrones is equal to the background loss.[27] In addition, frequency-dependent contributions to G'' and tan ϕ can also be present if further low- or high-frequency relaxation processes are in the proximity of the relaxation peak under consideration. As a result of this background loss, the half-width of a loss peak would be greater than the true value, which in turn can be obtained only when a correction for the background loss has been made.

In the face of the difficulty that the magnitude of the background loss cannot be a priori determined, one needs to develop criteria for or against the significance of its contribution to G'' and tan ϕ of a material. These we develop as follows:

(i) The presence of a frequency-independent background loss would raise the G'' and tan ϕ peaks in their entirety. Therefore, although the half-width of the peak without correction for a background loss would be greater than that after correcting for it, the two frequencies limiting the half-width of a peak would not satisfy the conditions of the two points of inflection (i.e., positive and negative maximum values of $(\partial \tan\phi/\partial \log \omega)_T$ or $(\partial G''/\partial \log \omega)_T$ when the background loss is present. These conditions would be satisfied when the background loss is absent.

(ii) The presence of a background loss would cause the values of $(\partial \tan\phi/\partial \log \omega)_T$ or $(\partial G''/\partial \log \omega)_T$ in the wings of the peak to approach zero when tan ϕ or G'' are greater than zero. Without the background loss the two values would approach zero only when tan ϕ and G'' approach zero.

(iii) Since a background loss raises tan ϕ or G'' and does not affect the G' values, it follows that, in its presence, the spectra of G' and G'' cannot be fitted to the same form of the stress relaxation function with the same set of parameters. Furthermore, the tan ϕ spectra calculated from the parameters of the fit of G' and G'' spectra to a relaxation function would not agree with the measured tan ϕ spectra.

Although all three of the above criteria can be critically examined when the G' and G'' spectra of a material are known in sufficient detail, it is the third criterion that is particularly useful if the data available are limited to only a few decades of frequency, as is the case here.

The analysis of the data in the preceding section and the evidence in Figures 1 and 2 and Tables I and II clearly demonstrate that the β-relaxation spectra of both G' and G'' can be fitted to a single set of parameters, and therefore according to criterion iii given above, the magnitude of the frequency-independent background loss must be negligible or zero. This conclusion is remarkable in view of the fact that justifications for the occurrence of frequency-independent background loss have been offered in terms of one-dimensional coupling of photon–phonon modes[26] with the applied stress or electric field, but without a crucial test for the existence of background loss in the manner discussed above.

3. Relaxation Rates. In Figure 3, the values of f_m determined from the G'' spectra of Figure 1b are higher than those determined from the G'' isochrones also shown in Figure 3. This difference arises mainly from the increase of ΔG with increasing temperature as is seen in Table II and Figure 8 and can be understood in terms of a relatively simple analysis of conditions at which $(\partial G''/\partial\omega)_T$ and $(\partial G''/\partial T)_\omega$ become zero in an isothermal and an isochronal measurement. In a fixed-temperature measurement, say at T_1 for a simplified condition for $\beta = 1$ (in eq 10), the peak in the G'' spectrum appears when $(\partial G''/\partial\omega)_T = 0$, or that in the equation

$$\frac{\tau_m \Delta G}{[1 + (\omega\tau_m)^2]^2}[1 - (\omega\tau_m)^2] = 0 \qquad (18)$$

when $\omega = 1/\tau_m$, where $\tau_m = \tau_0 \exp(E/RT_1)$, or $T_1 = E/R[\ln(1/\omega\tau_\infty)]$. But for a fixed-frequency measurement, say at ω, the peak in the isochrones of G'' against temperature occurs when $(\partial G''/\partial T)_\omega = 0$, or that when

$$\left(\frac{\partial \Delta G}{\partial T}\right)_\omega \frac{RT^2}{E}[1 + (\omega\tau_m)^2] = \Delta G[1 - (\omega\tau_m)^2] \qquad (19)$$

where

$$\tau_m = \tau_0 \exp[E/RT] \qquad (20)$$

If $(\partial \Delta G/\partial T)_\omega$ in eq 14 were equal to zero, the condition for $(\partial G''/\partial \omega)_T$ to be equal to 0 would be the same as for $(\partial G''/\partial T)_\omega = 0$; i.e., when $\omega = 1/\tau_m$ the isothermal and isochronal measurements would give the same value of τ_m at the same temperature. However, since $(\partial \Delta G/\partial T)_\omega > 0$, as is seen in Table II and Figure 8, the peak in an isothermal measurement would appear at a higher frequency than in the corresponding isochronal measurements as observed in Figure 3.

We now consider why the value of f_m determined from the G'' spectrum is higher than that determined from the tan ϕ spectrum, as is seen in Figure 3. For a dielectric relaxation process, McCrum, Read, and Williams[8] have discussed the reasons for this difference. For a mechanical relaxation process this difference is zero when $G_R = 0$ and increases as G_R increases in direct proportion to $(G_R/G_U)^{1/2}$. Alternatively speaking, when $B = 1$, G'', which is given by the equation

$$G'' = \frac{G_U - G_R}{1 + \omega^2\tau^2}\omega\tau \qquad (21)$$

reaches a maximum when $\omega\tau = 1$, and tan ϕ reaches a maximum value when $\omega\tau = (G_R/G_U)^{1/2}$ according to the equation

$$\tan\phi = (G''/G') = \frac{\omega\tau G_U - \omega\tau G_R}{G_U\omega^2\tau^2 + G_R} \qquad (22)$$

where

$$G' = G_R + \frac{(G_U - G_R)\omega^2\tau^2}{1 + \omega^2\tau^2} \qquad (23)$$

If G_R is several orders of magnitude less than G_U, as is the case for the α-relaxation process, eqs 21 and 23 imply that the value of f_m determined from the G'' spectrum would greatly differ from that determined from the tan ϕ spectrum. However, when $G_R \rightarrow G_U$, this difference approaches zero. In Table II, $(G_R/G_U)^{1/2}$ decreases from 0.763 at 213 K to 0.717 at 300 K for the β-relaxation process and therefore the difference between the $f_m(G'')$ and f_m(tan ϕ) seen in Figure 3 decreases with increasing temperature and is generally relatively less than that observed for the α-relaxation process.[29]

Despite our use of an alternative distribution function to more adequately describe the shape of the β-relaxation spectra, it is instructive to consider the various relaxation times obtained from the KWW function and their respective temperature dependence.

Figure 12 shows plots of the calculated characteristic time, τ_0, of eq 2, the average relaxation time, $\langle\tau\rangle$, calculated from eq 8, and τ_m ($=\omega_m^{-1}$) determined from the G'' relaxation spectra shown in Figure 1b. Since the value of $\langle\tau\rangle$ is dependent upon both β and the gamma function of β, it becomes increasingly more sensitive to errors in the value of β when β is low, as is the case here. For a temperature-independent value of β, $\langle\tau\rangle$ is higher than τ_0 by a factor $\Gamma(1/\beta)/\beta$ and the slopes of the Arrhenius plot of $\langle\tau\rangle$ and τ_0 are expected to be identical. Hoever, when β decreases with increasing temperature, the difference between $\langle\tau\rangle$ and τ_0 is greater at low temperatures than at high temperatures, and therefore, the activation energy for $\langle\tau\rangle$ becomes less than that for τ_0. Figure 12 shows this behavior, thereby underscoring a need for caution in both the use and comparison of activation energy values when β is temperature dependent.

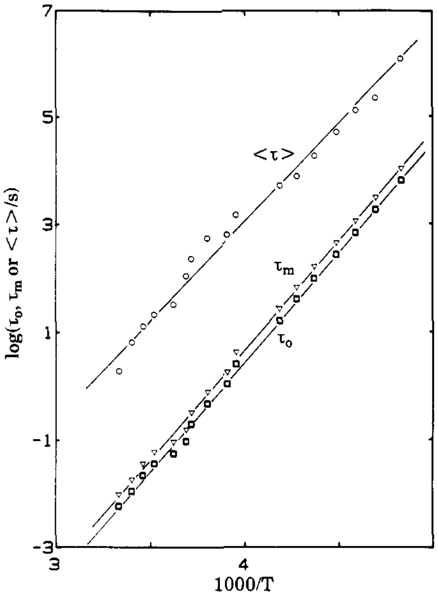

Figure 12. Relaxation time τ_m determined from the G'' spectra of Figure 1b (▽), the calculated characteristic time τ_0 (□), and the average relaxation time $\langle\tau\rangle$ calculated from eq 8 (○) plotted against the reciprocal temperature for the β-relaxation process in poly(methyl methacrylate).

The characteristic time τ_0 of eq 2 is generally lower than the τ_m obtained from the peak frequency of a relaxation spectrum; i.e., log (τ_0/τ_m) becomes progressively more negative as β decreases. Moynihan et al.[13] have given the characteristic features of the normalized complex quantities for the relaxation function of eq 1 for values of $0.3 < \beta < 1$.

By using the data given in Table 1 in ref 9, we extrapolate log $(\tau_0/\tau_m) \approx -0.22$ for $\beta = 0.16$; that is, τ_m should be 0.22 decades higher than τ_0. This is confirmed by our own calculations. A comparison of the two plots in Figure 8 shows that log $(\tau_0/\tau_m) \approx -0.23$ and the τ_m values seem consistently higher than τ_0 values by 0.23 decades of frequency. The agreement between the calculated (τ_0/τ_m) and experimental (τ_0/τ_m) even at a single temperature confirms the essential correctness of our procedure for the analysis as given in section IV here and our conclusion that the stretched exponential relaxation function is an appropriate description of the β-relaxation spectra.

4. Mechanical and Dielectric β-Relaxations. We now consider whether or not the dielectric and mechanical relaxations in PMMA are similar enough to admit to the same mechanism of localized rotational and translational diffusion. All modes of localized and long-range diffusion of a polymer chain that reorient an electric dipole couple with both the electric and stress fields applied for the study of the relaxation behavior. Nevertheless, when the rotational diffusion occurs about the C_{2v} axis that coincides with the dipole vector of a molecule, the dielectric measurements do not reveal a relaxation process but mechanical measurements do. Since all modes of motion of a polymer chain are not dielectrically active and when rotational diffusion occurs about a variety of different axes among which only a few reorient a dipole, the shape of the relaxation spectrum and the average rates of relaxation in a dielectric measurement differ from those in a mechanical measurement. A comparison of both the shape of the spectrum and the rate of relaxation measured in the two sets of measurements is, therefore, useful in studies of molecular relaxation phenomena. For this comparison, it is convenient to use the data on a dielectric study of PMMA over a wide frequency range which have been provided by Gomez-Ribelles and Diaz-Calleja in ref 27. Since it is difficult to analyze in detail all the relaxation spectra given in Figure 1 of ref 27, we chose a typical temperature of 253.1 K for the spectra in Figure 1, which is approximately in the middle of the temperature range of our study, and calculated $\beta = 0.19 \pm 0.02$ by using the procedure described above (although the data in ref 27 have been fitted to a Fuoss–Kirkwood distribution). Within the uncertainties of both the experiment and of our reading of the data in ref 27, $\beta = 0.17$ is indistinguishable from $\beta = 0.16 \pm 0.01$ at $T = 253$ K calculated for the mechanical spectra and given in Table I. Equally important is the observation evident in Figure 3 that the dielectric and mechanical relaxation rates are similar in the temperature range of their overlap and further that the mechanical relaxation rates linearly extrapolate into a high-temperature region to the values measured from dielectric relaxation. The similarity both in the shapes of the dielectric and mechanical relaxation spectrum and in the relaxation rates strongly suggests that the underlying mechanisms for the local relaxation of mechanical and electrical stresses in PMMA must be similar in their mathematical and physical descriptions.

There is a further point of interest that deals with the often-sought correspondence between the ϵ^* with J^* ($=G^{*-1}$) and M^* ($=\epsilon^{*-1}$)[28] with G^*. In the current literature, reviewed by Angell,[30] the electrical modulus (M^*) and the G^*, it is suggested, provide similar relaxation rates for molecular diffusion in amorphous solids, particularly ionic glasses. Therefore, the similarities between the shape of the dielectric (ϵ'' and not M^*) and mechanical (G'' and not J'') relaxation peaks and rates of the corresponding spectrum in PMMA seem at first surprising. We note that the $\Delta\epsilon$ or ($\epsilon_R - \epsilon_U$) for PMMA, which is between 1.6 and 1.8,[27] is relatively low and $\epsilon_U \approx 3$. From the phenomenological description given by McCrum, Read, and Williams,[8] we deduce that as $\Delta\epsilon \rightarrow 0$, the frequencies at which ϵ'', M'', and $\tan\phi$ reach their respective maximum values become progressively close to each other. For large values of $\Delta\epsilon$ the M'' spectrum appears at a much higher frequency than the $\tan\phi$ spectrum, which in turn appears at a much higher frequency than the ϵ'' spectrum. Thus for low values of $\Delta\epsilon$, the f_m determined from the ϵ'' and M'' spectra would be nearly the same and comparable to the f_m obtained from the G'' spectrum, as is found here.

V. Conclusions

The shape of the mechanical relaxation spectra of PMMA at temperatures below its T_g has been analyzed in terms of both a stretched exponential or Kohlrausch–Williams–Watts relaxation function and an alternative relaxation time distribution function. Both the height of the relaxation peak and the ΔG increase with increasing temperature due mainly to the increase in the number of chain segments that undergo thermally activated motions in the rigid amorphous matrix. The temperature variation of G_U, G_R, and β, the parameter for the KWW formalism seems contrary to our generally held notions of relaxation phenomena. An alternative relaxation time distribution function based upon a parameter to account for the departure of the spectra from a symmetrical distribution gives more meaningful values and the temperature dependence of ΔG, G_U, G_R, and the width of distribution. These indicate that the broad relaxation spectra are a manifestation of a distribution of free activation energy, entropy, and enthalpy for the β-relaxation in PMMA.

Several criteria for ascertaining the presence of a frequency-independent background loss, when used for the β-relaxation in PMMA, show that the background mechanical loss at $T < T_g$ is negligible or zero.

The mechanical and dielectric relaxation times for the β-relaxation in PMMA are identical as is the value of β for its relaxation spectra. These similarities mean that the underlying mechanism of localized motion involve virtually the same chain segments containing a dipole and that the heights of the intermolecular barriers for these localized motions are the same.

Acknowledgment. This study constitutes part of the activities of the "Groupe de Recherche-933 CNRS" (Relations Structure—Propriétés mécaniques des polymères). It was partly supported by a research grant from the Natural Sciences and Engineering Research Council of Canada. This work will be submitted as part of the thèse de Doctorat by E. Muzeau.

References and Notes

(1) Williams, G. In *Molecular Liquids, Dynamics and Interactions*; Barnes, A. J., Orville-Thomas, W. J., Yarwood, J., Eds.; Reidel: Dordrecht, 1954; p 239.

(2) Johari, G. P. In *Molecular Dynamics and Relaxation Phenomena in Glasses*; Dorfmüller, Th., Williams, G., Eds.; Lecture Notes in Physics No. 277; Springer-Verlag: Heidelberg, Germany, 1986; p 90.

(3) Johari, G. P. *J. Chem. Phys.* **1973**, *58*, 1766.

(4) Perez, J. *Rev. Phys. Appl.* **1986**, *21*, 93.

(5) Cavaillé, J. Y.; Perez, J.; Johari, G. P. *Phys. Rev. B* **1989**, *39*, 2411.

(6) Matsuoka, S.; Kwei, T. K. In *Macromolecules—An Introduction to Polymer Science*; Academic Press: NY, 1979; Chapter 6.

(7) Nowick, A. S.; Berry, B. S. *Anelastic Relaxation in Crystalline Solids*; Academic Press: NY, 1972. Nowick, A. S.; Berry, B. S. *IBM J. Res. Dev.* **1961**, *5*, 297.

(8) McCrum, N. G.; Read, B. E.; Williams, G. *Anelastic and Dielectric Effects in Polymeric Solids*; Wiley: London, 1967.

(9) Kohlrausch, R. *Pogg. Ann. Phys. Chem.* **1854**, *91*, 179.

(10) Kohlrausch, F. *Pogg. Ann. Phys. Chem.* **1863**, *119*, 337.

(11) Williams, G.; Watts, D. C. *Trans. Faraday Soc.* **1970**, *66*, 80.

(12) Lindsey, C. P.; Patterson, G. D. *J. Chem. Phys.* **1980**, *73*, 3348.

(13) Moynihan, C. T.; Boesch, L. P.; Laberge, N. L. *Phys. Chem. Glasses* **1973**, *14*, 122.

(14) Palmer, R. G.; Stein, D. L.; Abrahams, E.; Anderson, P. W. *Phys. Rev. Lett.* **1984**, *53*, 958.

(15) Montroll, E. W.; Bendler, J. T. *J. Stat. Phys.* **1984**, *34*, 129.

(16) Schlesinger, M. F.; Montroll, E. W. *Proc. Natl. Acad. Sci. U.S.A.* **1984**, *81*, 1280.

(17) Montroll, E. W.; Weiss, G. H. *J. Math Phys.* **1965**, *6*, 167.

(18) Ngai, K. L.; Rendell, R. W.; Rajagopal, A. K.; Teitler, S. *Ann. N.Y. Acad. Sci.* **1986**, *484*, 150.

(19) Dishon, M.; Weiss, G. H.; Bendler, J. T. *J. Res. Natl. Bur. Stand. U.S.A.* **1985**, *90*, 27.

(20) Bendler, J. T.; Schlesinger, M. F. *Macromolecules* **1985**, *18*, 591.

(21) Havriliak, S., Jr.; Negami, S. *Polymer* **1967**, *8*, 161.

(22) MacDonald, J. R. *J. Appl. Phys.* **1963**, *34*, 538.

(23) Starkweather, H. W., Jr. *Macromolecules* **1988**, *21*, 1798; **1990**, *23*, 328.

(24) Wehrle, M.; Hellmann, G. P.; Spiess, H. W. *Colloid Polym. Sci.* **1987**, *265*, 815.

(25) Rössler, E. *J. Chem. Phys.* **1990**, *92*, 5847.

(26) Amrhein, E. M.; Muller, F. H. *J. Am. Chem. Soc.* **1968**, *90*, 3146.

(27) Gomez-Ribelles, J. L.; Diaz-Calleja, R. *J. Polym. Sci., Polym. Phys. Ed.* **1985**, *23*, 1297.

(28) Macedo, P. B.; Moynihan, C. T.; Bose, R. *Phys. Chem. Glasses* **1972**, *13*, 171.

(29) Jourdan, C.; Cavaillé, J. Y.; Perez, J.; Monnerie, L.; Johari, G. P. *J. Polym. Sci., Polym. Phys. Ed.* **1987**, *25*, 1235.

(30) Angell, C. A. *Chem. Rev.* **1990**, *90*, 223.